MONITORING OF THE SNOW COVER WITH A GROUND-BASED SYNTHETIC APERTURE RADAR

Alberto Martinez-Vazquez[1], Joaquim Fortuny-Guasch[2] and Urs Gruber[3]

1. European Commission DG JRC, Ispra, Italy; alberto.martinez(at)jrc.it
2. European Commission DG JRC, Ispra, Italy; joaquim.fortuny(at)jrc.it
3. Swiss Federal Institute for Snow and Avalanche Research SLF, Davos, Switzerland; gruber(at)slf.ch

ABSTRACT

The feasibility of retrieving changes in the depth of snow cover by means of the LISA (LInear SAR) Ground-Based Synthetic Aperture Radar system has been investigated. The LISA instrument consists of a computer-controlled sledge moving along a linear axis 5 m long, a set of transmit and receive antennas, a network analyzer, and a C-Band amplifier. All the equipment is installed inside a temperature controlled container. The centre frequency used in the measurement campaign is 5.83 GHz (C-band), with a 60 MHz bandwidth. The resolution of a single SAR image is in the order of 6 m in azimuth and 2.5 m in range, while in the interferometric mode, the range resolution in the coherence images is below 2 mm in the line-of-sight direction. Typical image products of LISA are similar to those of space or aerial radar missions. The only particularity of LISA is that the image covers a much smaller area (a few square km). However, it has the advantage of providing images at a much larger acquisition rate (about some tens in a single day). Over several weeks this amounts to a very large time-series of radar images that gives the opportunity to assess the feasibility of using a GB-SAR (Ground Based Synthetic Aperture Radar) system to monitor structural changes of the snow cover. The availability of a sensor network and meteo stations on the slope gives the possibility of validating the retrieval scheme.

The retrieval techniques that are going to be assessed will be those previously developed for space-borne and air-borne SAR imagery. The two principal indicators of the structural changes in the snow cover are the interferometric phase and the coherence. Using the data acquired by the ground sensors, an inversion scheme to monitor the snow cover depth has been calibrated with available ground-truth data for various temporal windows spanning a few days. The results prove the linear relationship between the interferometric phase and the snow depth when the acquisition conditions permit a high coherence, confirming the potential use of a GB-SAR system to monitor the snow cover.

Keywords: Snow cover, LISA, GB-SAR, differential interferometry

INTRODUCTION

In the past few years, ground based synthetic aperture radar interferometry has proved its ability to monitor large man-made structures such as buildings, dams and bridges (1,2) as well as natural hazards like landslides (3). On the other hand, conventional space-borne SAR imagery has been used to map the snow cover as well as to model and forecast snow melt runoff (4). The work presented in this paper demonstrates the feasibility to monitor snow cover with techniques of space-borne SAR imagery, taking the advantages of ground based systems. The main advantage is the possibility to achieve a much higher acquisition rate, of the order of several images per hour (and not every 35 days as, for instance, with ERS). This results in a massive time series of radar images with high coherence. The trade off is a small covered area, typically a few square kilometres, which contrasts with the tens or hundreds of kilometres achieved with air-borne or satellite systems.

Within the framework of a scientific collaboration between the Joint Research Centre (JRC, Ispra) and the Swiss Federal Institute for Snow and Avalanche Research (SLF, Davos), in November 2003 the LISA instrument (LInear Synthetic Aperture Radar, linear SAR) was deployed in the Test

Site at Vallée de la Sionne. Since then the instrument has completed a 124 days field campaign for the winter 2003-2004, gathering nearly 6000 images at a rate of 1 image every 30 minutes. In the winter 2004-2005 campaign the instrument is working with an improved acquisition rate of 1 image every 10 minutes.

THEORY

The propagation of electromagnetic waves in snow is governed by the complex permittivity which is strongly dependent on the liquid water content. The penetration depth d_p at the wavelength λ_o can be estimated from the real ε' and imaginary ε'' parts of the complex permittivity according to:

$$d_p = \frac{\lambda_o \sqrt{\varepsilon'}}{2\pi\varepsilon''} \tag{1}$$

ε'' of dry snow at C- and L-band is of the order of 0.001 to 0.0001, whereas ε' depends only on the snow density (5):

$$\varepsilon' = 1 + 1.60\rho + 1.86\rho^3 \tag{2}$$

where ρ is specified in g/cm^3. This results in a typical penetration depth on dry winter snow of $d_p \approx 20$ m at C-band and $d_p > 50$ m at L-band. The dielectric losses of wet snow, on the other hand, are large and the typical penetration depth of wet snow containing several per cent of liquid water by volume is of the order of few centimetres only (6).

The InSAR (Interferometric SAR) snow depth retrieval algorithm used in this work exploits the large penetration depth in dry snow, taking into account that the main contribution of backscattering from ground covered by dry winter snow stems from the ground surface. It is assumed that the dielectric properties are constant all over the snow cover. In the case in which this is not true, an equivalent single dielectric constant should be computed considering the geometry and properties of the different layers (this is outside the scope of this work).

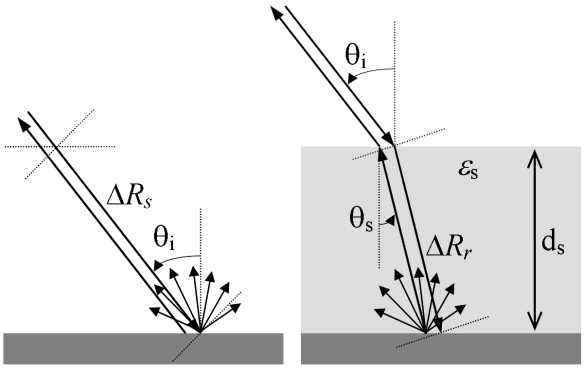

Figure 1: Propagation path of microwaves without and with snow.

Synthetic aperture radar interferometry is based on the phase comparison of a pair of complex coherent radar images of the same scene taken in different instants of time. Let d_s denote the depth of the snow layer and $2{\cdot}\Delta R_r$ the distance in the snow layer travelled by the radar pulse at some instant as shown in Figure 1. After some minutes, during which the snow depth may have changed, the radar sends another pulse. Let the new snow cover depth be d_s' and the new distance travelled by the radar signal be $2{\cdot}\Delta R_r$'. This path difference, in the form of a phase shift, is actually the information measured by the radar with resolution of millimetres in C-band ($\lambda_0 \approx 5$ cm). For calculating the phase shift in snow, the different propagation constants between air and snow (ε_0 and ε_s) have to be taken into account in addition to the differences in the geometric path (ΔR_r *and* ΔR_r'). This change in the target causes the following phase shift (7):

$$\Delta\phi_S = -\frac{4\pi}{\lambda_o}\Delta d_s\left(\cos\theta_i - \sqrt{\varepsilon_s' - \sin\theta_i^2}\right) \quad (3)$$

Thus, the phase shift $\Delta\phi_s$ and the differential snow depth Δd_s can be linked by a very simple linear relationship depending on three variables: the central wavelength λ_o, the physical properties of the snow ε_s' and the incidence angle θ_i. When the area under study is small enough, the incidence angle and the snow permittivity can be considered constant, allowing the reduction of the above-mentioned three variables to a single constant α. Because the phase shift values come from differential measurements ($\Delta d_s = d_s - d_s'$), an offset constant needs to be added to the previous equation in order to calibrate the results to absolute snow heights:

$$d_S = d_{offset} + \alpha \cdot \Delta\phi_{snow} \quad (4)$$

INSTRUMENT DESCRIPTION

The system used to monitor the snow cover in our campaign is a ground based linear SAR (LISA) fully developed and built in the Joint Research Centre (Ispra, Italy). The radar is mounted in a temperature-controlled trailer to easily transport and deploy it. The heart of the instrument is a vector network analyzer, which is used to generate the stepped-frequency continuous wave (SF-CW) radar pulses and receive the coherent responses. A sled carrying the network analyzer and the antennas (one for transmission and one for reception) is slid along a rail 5 m long in order to synthesize a linear aperture such that the azimuth resolution is obtained. This movement is directed by a linear positioner by means of a serial interface and the appropriate control software. A mobile phone is used to remote control the automatic measurements through the public GSM (Global System for Mobile Communications) network. Finally a personal computer operates all the systems and is used also for data archiving and processing.

The instrument has been working for the winter 2003-2004 in vertical polarization with a central frequency of 5.83 GHz (C-band). The bandwidth generated has been of 60 MHz, sampled in 1601 points. The aperture synthesized along the *x* axis or azimuth direction was 3.5 m long in 251 steps. This gives the following spatial resolution in azimuth (Δx) and range (Δr):

$$\begin{aligned} \Delta x &= \frac{\lambda_o \cdot R}{2L} \approx 7.3 \text{ m} \\ \Delta r &= \frac{c}{2B_f} \approx 2.5 \text{ m} \end{aligned} \quad (5)$$

In the above formulas c is the speed of light, B_f the frequency band, R the average radar-to-target distance and L the synthetic aperture. The radar image obtained by the GB-SAR system is formed by means of a time-domain algorithm (8).

TEST SITE

The before mentioned GB-SAR system has been used to monitor a Swiss test-site for avalanche experiments managed by the Swiss Federal Institute for Snow and Avalanche Research (SLF, Davos). The site is located in the Sion valley, in the Canton Valais, and consists of a concave shaped channel of 1200 m vertical drop and an average slope of 27 degrees. The avalanche path length is 2.5 km, starting from the highest elevation level at 2650 m and finishing at the level of 1450 m.

Several instruments are available in the test site. Two meteorological stations provide data concerning temperatures, wind speed and direction as well as snow height. Three pairs of FM-CW (Frequency Modulation Continuous Wave) radars are located in the avalanche corridor to determine the height of the avalanche, its speed, turbulences and density. Two geophones make it possible to automatically start the measuring equipment when spontaneous avalanches occur. For impact studies a narrow wedge of steel construction 20 m high is in the middle of the avalanche track. It is equipped with force transducers and pressure and strain gauges. On the side of the py-

lon, snow height sensors have been installed. These sensors allow the avalanche flow height to be determined through contact with the moving snow mass. Set at intervals of 25 cm along the pole axis, these sensors record the height of the flow up to a height of about 8.5 m (9).

In order to observe the avalanche under the best possible conditions, a bunker is located in the mountain opposite to the corridor 350 metres above the lower level of the valley. It is also used for recording the measurements made in the corridor and to provide the power energy to the LISA system.

The LISA system was deployed by a helicopter in the mountain opposite to the avalanche corridor at an approximate level of 1800 m. In that way the instrument has direct visibility of the scenario, covering a cross range section of more than 2200 m. The distance of the instrument to the slope ranges approximately from 1000 m to 2900 m, hence, the area covered by the radar is nearly 2 km by 2 km. The local incidence angle of the radar with respect to the normal of the slope in the far field ranges from 33 to 80 degrees. Besides the snow cover, which was monitored daily, several avalanches in the winter 2003-2004 campaign, some natural and one artificially released, have been properly recorded by the LISA system.

PROCESSING METHODOLOGY

The algorithm proposed is divided into four steps as follows:

Coregistering the images

The coregistering process consists in minimizing the atmospheric effects present in the raw data sets due to changes in the air refractivity (caused by variations in the air's temperature and humidity) during the radar scanning. This is the major source of temporal decorrelation of the acquired images, that translates into a rotation in the azimuth direction of the focused images when these effects are linear.

The process is done by comparing all the power images in the data set with a reference one, and adjusting these images to maximize their cross-correlation in azimuth with the reference one. Usually the first file in the directory is used as a reference, although the only relevant criterion is having a reference image with good signal to noise ratio.

First, the raw data in the azimuth dimension is zero padded in order to increase the sampling rate in the transformed domain, achieving a coregister displacement resolution of the order of 1/10 pixel. Then, in the transformed domain the shift displacement between images is computed as a weighted sum among the range dimension of the correlation indexes with the correlation values, giving in that way a higher weight to pixels with higher power. The coregistering operation in the transformed domain is equal to the convolution of the signal with a delta function. In the original domain, the shift displacement is converted into a phase rotation by means of a complex exponential factor, and the inverse rotation is applied to the raw images in order to correct for the temporal decorrelation.

Selection of the master image

The computation of an interferogram (next step) requires the definition of a master image. Then, the rest of images are operated against that master to obtain every interferogram. Two criteria have been found to be good indicators of the quality for an image to be master: a higher value in the averaged coherence, and a lower value in the averaged phase standard deviation. These two factors present also a high degree of correlation in the data sets analyzed up to the present moment.

This step needs a brute-force analysis that is very time consuming, since all the possible images in the data set are tested as candidates for master image. For the data gathered in the winter campaign 2003-2004 we have observed that the coherence values are high enough to allow good interferograms with little dependency (0.20 radians of almost constant phase offset) on the master image selected.

Computation of interferograms

The interferogram is the basic operation that provides the phase shifts used in Eq. (4). It is defined by the complex correlation function γ, and is computed pixel by pixel according to the following equation:

$$\gamma = \frac{\langle I_1 \cdot I_2 * \rangle}{\sqrt{\langle |I_1|^2 \rangle \langle |I_2|^2 \rangle}} \tag{6}$$

The averaging operator $\langle \cdot \rangle$ has been implemented as the two-dimensional convolution of the power signal with a square matrix of size 3×3 with all its components equal to one. The * operator represents the complex conjugate of the signal.

From the interferogram two products are obtained: the coherence (absolute value of γ), and the interferometric phase (angle of γ). Although real phases can range between -∞ and ∞, the phase computed as the arctangent of the complex interferogram can only range, by definition, between -π and π. Thus, a two-dimensional phase unwrapping algorithm is needed in order to correct this effect. The algorithm implemented is an FFT-based solution of the unweighted least-squares phase unwrapping problem, that is simple to implement and computationally very efficient because it avoids the loops of the path-following methods (10).

Calibration

Once an unwrapped interferometric phase is available for the area under study, the average value over all the pixels in the image is computed $\Delta\phi_s$. Repeating that process for every image acquired in a whole day, a time-series of averaged phases is obtained. Such a series suffers again from phase wrapping, so a one-dimensional phase unwrapping algorithm needs to be applied. In that case the procedure is much simpler, since the procedure simply changes absolute jumps greater than π to their 2π complement.

Nevertheless, this step is very sensitive, since jumps of 2π rad correspond to displacements of only 5 cm in C-band in the line-of-sight direction. During a moderate snow fall it is easy to achieve such increment in the snow cover between two images acquisitions, so jumps bigger than 2π can confuse the unwrapping algorithm. To minimize this effect, for the winter campaign 2004-2005 the acquisition time has been reduced from 30 to 10 minutes.

Finally, the unwrapped phase is smoothed in order to reduce the irregularities of the process, and then translated into snow height according to Eq. (4). Since the process has been applied to whole days' data sets, the calibration parameter d_{offset} is directly the snow height provided by the meteorological station in the first measurement of the day (at 00:01h), or the last value estimated in the previous day at 23:59h. On the other hand, the parameter α has been experimentally found to be between 2 and 2.5 after having trained the algorithm with ground-truth data of previous days. Note that here it is assumed that the snow permittivity suffers little variation between the moment of calibration of the parameter α and the time window when it is later used.

RESULTS

In Figure 2 can be seen an ortho-photo of the test site besides a radar image of the coherence. Note that the black zones in the radar image correspond to shadow areas that the radar cannot reach, and thus there is no backscatter signal. Observing the photo it is clear that these zones correspond to changes in the slope where the radar has no direct visibility.

On the other hand the light squares on the top-right corner represent the zone of interest where the results have been computed and averaged. That zone corresponds to a focused image of 21×21 pixels, covering an area of approximately 150×50 metres. This zone has been selected to be approximately at the same level as the meteorological station providing the ground truth data, so the snow conditions will be similar on both sites although they are separated 2 km.

Using as a master the first image of the day, interferograms with the rest of the images in the day have been computed, providing snow height profiles of complete days at intervals of 30 minutes.

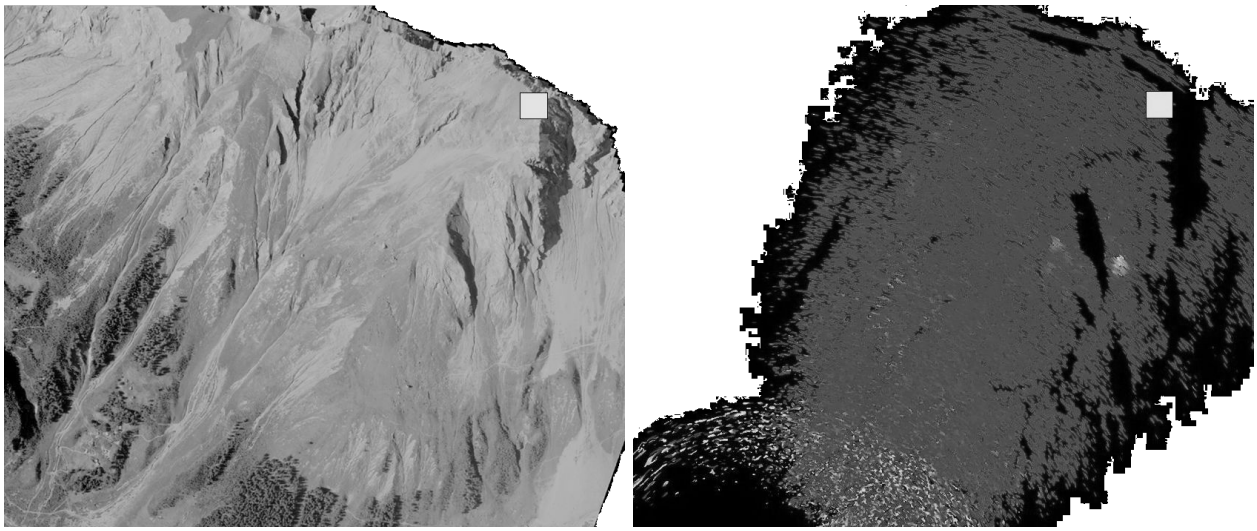

Figure 2: Ortho-photo and radar image of the test site.

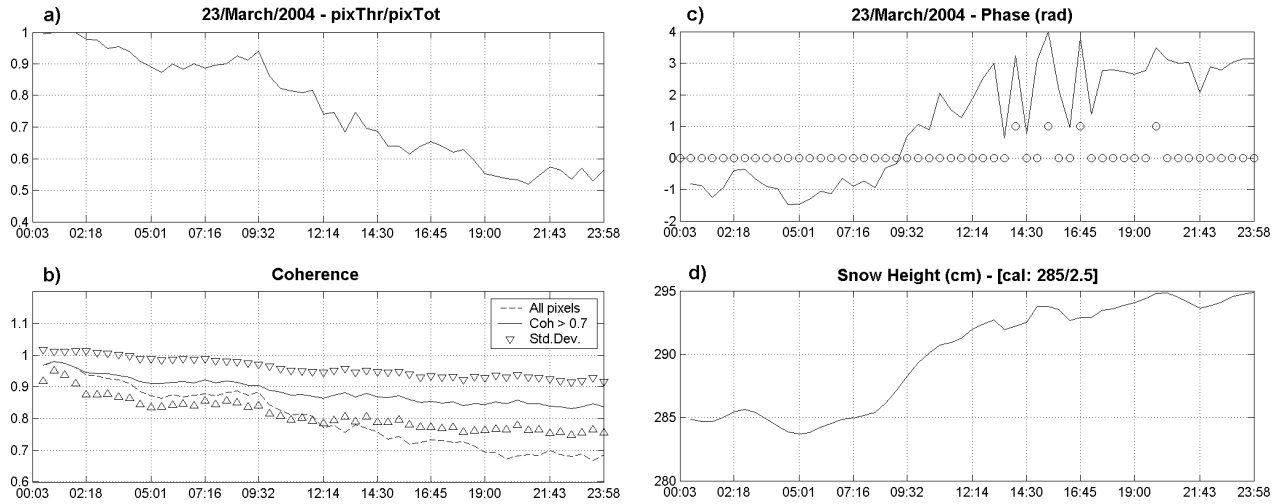

Figure 3: Computed data for the 23 March 2004.

In Figure 3 are shown the computed results for the 23 March 2004, where the x-axis is always the time of the day in the format HH:MM. The subplot a) represents the coefficient of pixels with coherence greater than the threshold introduced as a parameter (typically equal to 0.7) with respect to the total number of pixels in the image. The subplot b) shows with a continuous line the average coherence of the pixels with coherence greater than the threshold, while the discontinuous line represents the average coherence of all the pixels in each image. A couple of triangles (one pointing up and the other one pointing down) all along the continuous line represent the standard deviation of the coherence in every point. Since the phase results are averaged only in the pixels with coherence greater than the threshold, these two graphics summarize the quality of the results retrieved. It should be also noted how the coherence decreases with time within the same period. This imposes a temporal window of approximately one day for the temporal extension of the results.

On the other column, the subplot c) is the superposition of the unwrapped interferometric phase together with the unwrapping 2π factors (these factors are the number of wrappings of the phase and are used to unwrap it), while the subplot d) is the snow height retrieved from equation (4).

Note that the snow profile is a smoothed version of the previous interferometric phase. The values between brackets (285 and 2.5) are the calibration parameters, d_{offset} and α respectively.

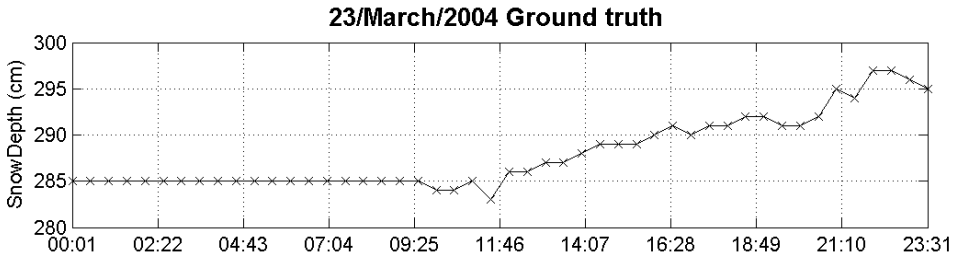

Figure 4: Ground-truth data for the 23 March 2004.

Figure 4 shows the ground-truth data gathered by the reference meteo station the same day. It can be seen that the shape as well as the absolute values match the estimated snow height in Figure 3d, with an average error of 2.4 cm and a standard deviation of 2.1 cm. Nevertheless, there are some noisy phase values in the Figure (3-c) between 12:30h and 17:00h that should be further studied in order to determine which kind of phenomenon is happening to disturb in such a way the phase.

Figure 5 presents similar results for the 6 April 2004. In this case, the coherence decreases slowly with time, as can be seen in the subplots a) and b). However, the interferometric phase in the subplot c) is much smoother than the one shown in the Figure 3c. This is a good quality indicator for the estimated snow height in that case, since it assures that the one-dimensional phase unwrapping has been applied without ambiguous jumps bigger than 2π.

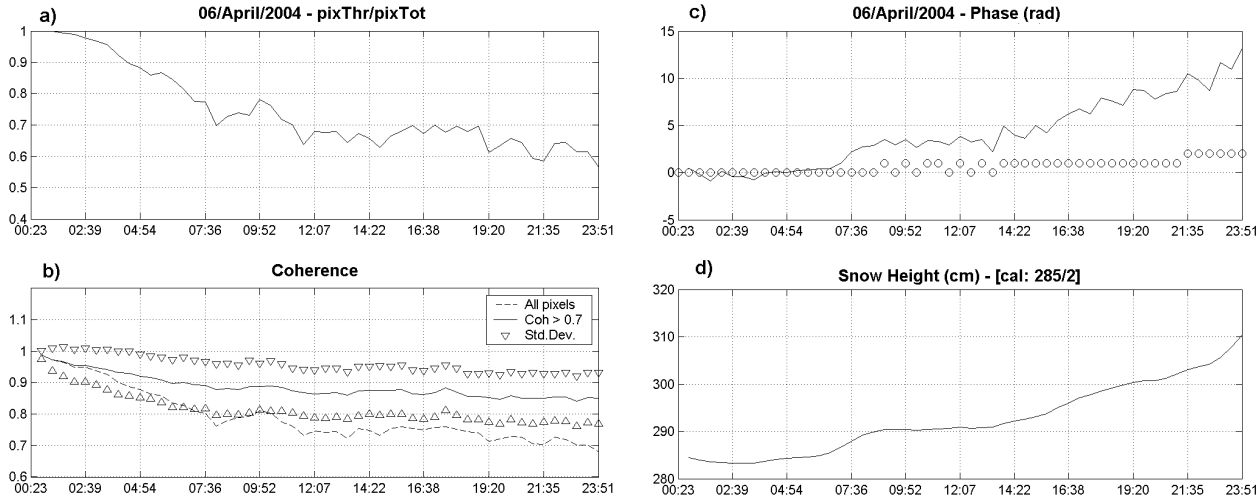

Figure 5: Computed data for the 6 April 2004

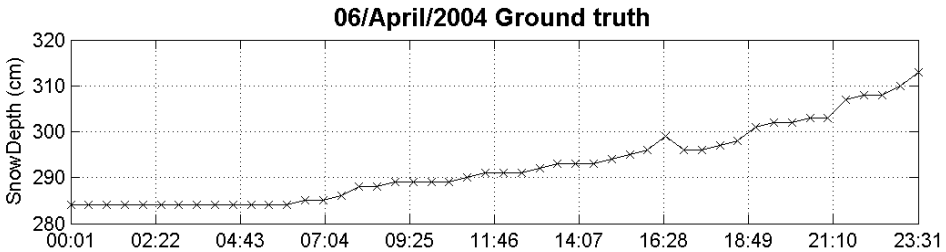

Figure 6: Ground-truth data for the 6 April 2004

The ground data shown in Figure 6 confirm the before mentioned quality factor. Actually, the matching between the estimated snow height in the Figure 5d and the meteo data is almost perfect, both in shape and in absolute values. The mean error in this case is 1.4 cm, with a standard deviation of 1.2 cm.

CONCLUSIONS

A dry snow height retrieval algorithm has been presented and validated through data gathered with a ground-based synthetic aperture radar in the test site Vallée de la Sionne. The main advantage of ground based systems is the high coherence of the interferograms, which translates into accurate snow depth profiles along one whole day with a single calibration at the beginning of the period under study. The use of a GB-SAR allows the monitoring of steep slopes where in-situ sensors are difficult to be installed and can be easily destroyed in case of avalanches.

Some improvements are still under investigation, as for example the extrapolation of the presented inversion scheme both in time and space. In this respect, the retrieval algorithm should be extended to the whole area illuminated by the radar and not only to the small region of interest used until now. The extension of the data sets from one day to larger periods of time also needs to be studied. With the use of two receiving antennas it is expected to generate a time series of digital terrain models (DTM) of the test site, and from them determine and assess the volume of the snow displaced in the avalanches. Finally, a deeper study of the images acquired during the natural and artificial avalanches may lead to the identification of some new precursors of avalanches based on ground-based SAR imagery.

REFERENCES

1 Pieraccini M, D Tarchi, H Rudolf, D Leva, G Luzi & C Atzeni, 2000. Interferometric radar for remote monitoring of buildings deformations. Electronic Letters, 36(6): 569-570

2 Tarchi D, H Rudolf, G Luzi, L Chiarantini, P Coppo & A J Sieber, 1999. SAR interferometry for structural changes detection: A demonstration test on a dam. International Geoscience and Remote Sensing Symposium, IGARSS '99, 1522-1524

3 Leva D, G Nico, D Tarchi, J Fortuny-Guash & A J Sieber, 2003. Temporal analysis of a landslide by means of a ground-based SAR interferometer. IEEE Transactions on Geoscience and Remote Sensing, 41: 745-752

4 Jiancheng Shi, J Dozier & H Rott, 1994. Active microwave measurements of snow cover progress in polarimetric SAR. International Geoscience and Remote Sensing Symposium, IGARSS '94, 4: 1922-1924

5 Matzler C, 1996. Microwave permittivity of dry snow. IEEE Transactions on Geoscience and Remote Sensing, 34(2): 573-581

6 Rott H, T Nagler & R Scheiber, 2003. Snow mass retrieval by means of SAR interferometry. In: 3rd FRINGE Workshop (European Space Agency ESA)

7 Guneriussen T, K A Hogda, H Johnsen & I Laukknes, 2001. InSAR for estimation of changes in snow water equivalent of dry snow. IEEE Transactions on Geoscience and Remote Sensing, 39(10): 2101-2108

8 Fortuny J & A J Sieber, 1994. Fast algorithm for near-field synthetic aperture radar processor. IEEE Transactions on Antennas and Propagation, 42: 1458-1460

9 Dufour F, U Gruber, B Sovilla & P Bartelt, 2004. A new Swiss test-site for avalanche Experiments in the Vallée de la Sionne / Valais (Swiss Federal Institute for Forest, Snow and Landscape Research, Davos, Switzerland)

10 Ghiglia D C & M D Pritt, 1998. Two-Dimensional Phase Unwrapping. Theory, Algorithms and Software (John Wiley & Sons), 188-195